Saulino *et al. Fire Ecology (2025) 21:41*
https://doi.org/10.1186/s42408-025-00382-3

Fire Ecology

ORIGINAL RESEARCH

Open Access

Has the tortoise scale exacerbated fire severity in Mediterranean stone pine forests?

Luigi Saulino[1*], Antonio Pietro Garonna[1], Francisco Castro Rego[2], Angelo Rita[1], Alessandro Aquino[1], Greta Liuzzi[1], Riccardo Fornaro[1], Enrica Pinelli[1], Roberto Silvestro[3], Sergio Rossi[3] and Antonio Saracino[1]

Abstract

Background Introduction of non-native insect species and extreme wildfire events threaten terrestrial ecosystems and their services worldwide. However, the effect of invasive sap-feeding insect species outbreaks on fire severity is poorly understood, particularly regarding their effects on fire behavior and the probability of crown fire ignition. We set up two experimental designs to investigate how the alien tortoise scale *Toumeyella parvicornis* influenced fire behavior dynamics and canopy surface reflectance in Mediterranean *Pinus pinea* stands that were severely burnt in the summer of 2017. We combined Rothermel's model for fire surface spread and Van Wagner's crown ignition model to simulate fire behavior and employed data from the Landsat 8 collection to detect canopy wilt symptoms related to the multivoltine *T. parvicornis* abundance.

Results Simulating fire behavior in single-story *P. pinea* thinned and unthinned stands indicated that all the predicted fires were surface fires. Uncertainty analysis of the canopy fuel attribute model inputs revealed that fires in thinned stands were entirely classified as surface fires. In contrast, only 62.7% were surface fires in unthinned stands, whereas 37.3% were categorized as conditional fire types. Among the Landsat reflectance bands, only the NIR, green, and SWIR 2 were sensitive to the abundance of *T. parvicornis*. Based on these sensitive bands, two-band NIR-multiplied vegetation indices were significantly associated with the abundance of *T. parvicornis* from the fall generation onward when sooty mold consistently covered the canopy needles.

Conclusion The divergence between observed and predicted fires in pine stands highlights the need to investigate the processes and variables linked to *T. parvicornis* feeding activity on *P. pinea* trees to enhance fire behavior prediction. Therefore, understanding how insect outbreaks can modify fire behavior in pine stands is crucial for effective management at the local and landscape levels. Identifying the vegetation index based on sensitive bands represents an essential step toward the early recognition of insect outbreaks on a large spatial scale.

Keywords Canopy fuels, Crown fires, Extreme wildfires, Fire behavior, Fire modeling, Forest structure, Insect outbreak, Sap-feeding insect, *Pinus pinea*, *Toumeyella parvicornis*

Resumen

Antecedentes La introducción de especies de insectos no nativos y los eventos de incendios de comportamiento extremo amenazan los ecosistemas terrestres en todo el mundo. Sin embargo, los efectos del estallido de insectos chupadores de savia no nativos, sobre la severidad de los incendios es poco entendido, particularmente en relación a sus efectos en el comportamiento del fuego y en la probabilidad de ignición de las coronas. Establecimos dos

*Correspondence:
Luigi Saulino
luigi.saulino@unina.it
Full list of author information is available at the end of the article

diseños experimentales para investigar cómo la especie exótica "escama de tortuga del pino" (*Toumeyella parvicornis*) influencia la dinámica del comportamiento del fuego y la reflectancia en la superficie del dosel en rodales de pino Mediterráneo (*Pinus pinea)* que fueron severamente quemados en el verano de 2017. Combinamos el modelo de propagación de fuegos superficiales de Rothermel y el modelo de ignición de coronas de Van Wagner, para simular el comportamiento del fuego y empleamos colecciones de datos del Landsat 8 para detectar síntomas de marchitez relacionados con la abundancia de la especie multianual *T. parvicornis*.

Resultados La simulación del comportamiento del fuego en rodales coetáneos de *Pinus pinea* raleados y no raleados indicaron que todos los fuegos pronosticados fueron superficiales. Los análisis de incertidumbre de los modelos conteniendo los ingresos de datos de diferentes atributos revelaron que los fuegos en rodales raleados fueron todos clasificados como fuegos superficiales. En contraste, solo el 62,7% de los fuegos fueron superficiales en rodales no raleados, mientras que el 37,3% fueron categorizados como tipos de fuegos condicionales. Dentro de las bandas de reflectancia del Landsat, solo el NIR, green, y SWIR 2 fueron sensibles a la abundancia de *T parvicornis*. Basados en esas bandas sensibles, dos índices de bandas NIR- y vegetación múltiple fueron asociados significativamente con la abundancia de *T. parvicornis* desde la generación nacida en el otoño en adelante, cuando la fumagina cubrió consistentemente las acículas del dosel.

Conclusiones La divergencia entre fuegos observados y pronosticados en rodales de pino subraya la necesidad de investigar los procesos y variables ligados con la actividad de alimentación de *T. parvicornis* sobre árboles de *Pinus pinea* para aumentar la predicción sobre el comportamiento del fuego. Por lo tanto, el entender cómo el estallido de insectos puede modificar el comportamiento del fuego en rodales de pino, es crucial para el manejo efectivo a niveles locales y de paisaje. Identificar el índice de vegetación basado en bandas sensibles representa un escalón esencial hacia el reconocimiento temprano del estallido de insectos a grandes escalas espaciales.

Background

Wildfires and insects are interacting components of forests worldwide, shaping these ecosystems at the local and landscape scales (Turner 2010; Chuvieco et al. 2021; Pausas and Keeley 2021). Although natural fires, independent of humans, shape forest species' composition and stand structure, affecting their functioning and resource availability (Bowman et al. 2020), human activities have profoundly shaped current fire disturbance regimes worldwide (Kelly et al. 2023). Consequently, the frequency of large and extreme wildfires in both non-fire and fire-prone ecosystems has increased significantly (Tedim et al. 2018; Cunningham et. al 2024), exacerbating their socioeconomic impact (Wang et al. 2018). Simultaneously, the current global market practices have contributed to introducing non-native and invasive insect species and their uncontrolled spread (Roques et al. 2020; Canelles et al. 2021; Garonna et al. 2018). Given the impacts of climate change, the frequency of extreme wildfires and the spread of invasive insects are expected to increase in the European Mediterranean region, along with their ecological and socioeconomic impacts (Galizia et al. 2021; Forzieri et al. 2023). Depending on their interactions, fire-invasive insect outbreaks can amplify the extent and severity of fires (Kane et al. 2017), thereby deteriorating ecosystem services (Cervelli et al. 2022; Silvestro et al. 2021; Misseyanni et al. 2025). Although insects represent a large part of the alien fauna and are among the taxa with the highest rate of introduction worldwide (Pyšek et al. 2010; Kenis et al. 2009), in the Mediterranean area, they have received less attention regarding their interaction with wildfire disturbances and their effects on fire behavior and severity.

In contrast, the interactions between native insects and fires in North American coniferous forests have been extensively studied, with contrasting results often attributed to variations in the spatiotemporal scale of the analysis (Meigs et al. 2015 and references therein). Insects acting as the main drivers of wildfire interactions are xylem, phloem, and foliage feeders (Canelles et al. 2021). Insect feeding strategies modify the stand structure of forests and biophysical properties of fuels, determine tree mortality, unbalance the ratio between live and dead aboveground fuel components, and modify the dead fuel accumulation rate, horizontal and vertical connectivity of fuels, and flammability of canopy leaves by reducing the moisture content (Rego et al. 2021a). Such fuel alterations amplify the fire susceptibility of forest vegetation and, subsequently, the behavior and severity of fires (Jolly et al. 2012; Kane et al. 2017). However, to our knowledge, little is known about the interaction between wildfire disturbances and sap-feeding insect outbreaks in *P. pinea* forest ecosystems of the Mediterranean basin, particularly regarding their effects on fire behavior and the probability of crown fires.

Toumeyella parvicornis is a soft-scale insect native to the Nearctic region that develops on specific *Pinus* species. In its native range, the primary pine tree host

species are *P. banksiana* and *P. sylvestris* (Clarke 2013). Outside its native range, it was observed on *P. caribaea* in the Turks and Caicos Islands, while in Southern Mediterranean Europe, large populations of these soft-scale insects developed on *P. pinea* rather than on other *Pinus* species (Garonna et al. 2018). Climatic conditions determine the number of generations that *T. parvicornis* completes each year. While toward the northern limit of its native range in the USA and Canada, *T. parvicornis* is univoltine with one complete generation per year (Cooper and Cranshaw 2004), outside its native range it becomes multivoltine completing at least three generations, partially overlapping, on *P. pinea* trees in Southern Mediterranean Europe (Garonna et al. 2018). The tortoise pine scale has received significantly less attention regarding their impacts on ecosystem patterns and processes than other insects, such as bark beetles (e.g., *Dendroctonus* spp. and *Ips* spp.). Even less research has focused on its interactions with wildfires and fire behavior. *T. parvicornis* feeds on the phloem sap of its host tree species, extracting nutrients from the diluted plant sap, while filtering excess water and sugars and discarding honeydew (Douglas 2009; Garonna et al. 2018). On *P. pinea*, large populations of *T. parvicornis* nymphs and adult females feed on the needles and current-year twigs, leading to crown yellowing, premature needle loss, and dieback of branches (known as flagging). The large quantities of excreted insect honeydew cover the host plants (including twigs, branches, and stem bark) and drip over all surfaces below the infested trees, such as litter and understory crowns when present. Although there is well-established knowledge that insect attack (e.g., bark beetles) leads to the accumulation of dead fuels, and then an increase in wildfire susceptibility, to our knowledge, no evidence of fuel modification by sap-feeding soft-scale insect outbreaks has been reported as the main driver of fire-insect interaction.

Over the last decade, wildfire events have blazed forest ecosystems at unprecedented rates of spread, intensity, and extension (Pais et al. 2023). Although fire regimes have historically been depicted in Eurasia (Pausas 2022), recent global events are emerging as novel extreme wildfires associated with a higher frequency than expected (Duane et al. 2021), posing serious risks to human health and property (Knorr et al. 2016; Xu et al. 2020). In 2017, extreme wildfires spread worldwide, causing extensive and severe fires in natural and artificial forests (UNEP 2022). In southern Italy, the high-severity wildfires experienced in 2017 in Mediterranean stone pine (*Pinus pinea* L.) forests have been only hypothetically linked to the non-native invasive pine tortoise scale (*Toumeyella parvicornis* Cockerell; hereinafter TP) insect species (Saulino et al. 2020). In Southern Italy, *T. parvicornis* was documented for the first time in 2014 in isolated *P. pinea* urban trees (Garonna et al. 2015); since 2015, it has rapidly spread in stone pine forest stands outside the urban environment (Garonna et al. 2018; Nicoletti et al. 2024; Niccoli et al. 2024). To our knowledge, besides the link with wildfires suggested by Saulino et al. (2020), invasive-scale insect species (Hemiptera: Coccidae) have never been related to wildfires inside or outside the native range of conifer forest species; this suggests that research studies are needed to fill this gap, fully understand fire-invasive insect-scale interactions, and incorporate them into fire behavior simulation modeling.

However, from a fire behavior perspective, the near-ground accumulation of flammable and volatile gases (e.g., biogenic volatile organic compounds; pyrolysis volatile products) produced during wildfire propagation, combined with complex topography (e.g., thalwegs and canyons) and weak wind conditions, has been associated with blowup or eruptive fire types (Viegas and Simeoni 2011). This unpredictable and hazardous eruptive fire behavior can arise when a cloud of volatile gases from incomplete combustion or heated vegetation fuels accumulates near the ground, where the gas concentration can reach the lower flammability limit (Chetehouna et al. 2014). Under these conditions, eruptive behavior determines a sudden and rapid acceleration of the surface rate of spread in the flaming front, with high-energy release and heat convection development, which has often been reported as the leading cause of most firefighter losses (Barboni et al. 2011). Although eruptive behavior has been frequently described as a fast and unexpected transition from a low-intensity surface fire to a canopy fire (Butler et al. 1998), it may also occur in a single layer of fuel (Viegas and Simeoni 2011). Nevertheless, insufficient knowledge about eruptive fire behavior hinders modeling or replicating it at the field scale (Rego et al. 2021b). Therefore, further research is warranted to identify the variables and factors involved in the eruptive behavior of forest fires and their potential interactions with insect-feeding activity.

Although insect outbreaks are traditionally monitored using field surveys, promptly monitoring large areas is not feasible with current high outbreak levels. Satellite remote sensing has long been used for insect spread assessment and monitoring (Tuominen et al. 2009) and is a key tool for detecting large-scale spatial distributions. Nevertheless, insect detection is challenging due to the infestation cycle's complexity, the cryptic behavior of several species (Rhodes et al. 2022), and intricate community and plant–insect relationships (Pincebourde et al. 2017). In this regard, a saprobe fungal group called sooty mold, which creates a black superficial encrustation of dense and dark hyphae on the host tree and all surfaces

below (Chomnunti et al. 2014), has been recorded on honeydew excreted by TP populations since the end of 2016 (Garonna et al. 2018). These sooty mold fungi have frequently been linked to changes in canopy tree reflectance signals in evergreen broad-leaved (Fletcher 2005; Gausman and Hart 1974) and evergreen conifer trees infested with scale insects (Olsson et al. 2012). Finding reflectance bands where only TP abundance and related infestation effects act as the dominant factors influencing the variation in canopy spectral reflectance would be helpful for practical and early detection.

Furthermore, because canopy trees show no significant and visible changes in the first stages despite the trees being already infested, understanding which infestation stages can be detected promptly helps to plan management activities to control and mitigate large-scale insect outbreaks. Aiming to understand the mechanisms of two chronologically independent events—the wildfires that occurred in 2017 in a Mediterranean *P. pinea* forest, which severely burned over 60% of its total surface (973 ha), and the pre-fire invasion of the alien insect pest TP started in 2015—we studied, at local scale, (*i*) how TP outbreaks could have mechanistically affected fire behavior, and (*ii*) whether the satellite surface reflectance bands are the most sensitive to highlight TP decline symptoms. Therefore, we first quantified fire behavior by employing Rothermel's surface fire model (Rothermel 1991; 1972) in combination with Van Wagner's crown ignition model in two different *P. pinea* stand types with different management regimes (thinned and unthinned) (Van Wagner 1993; 1977). For fire behavior simulation, the boundary conditions (topography and fire weather) and pre-fire fuel conditions were referred to as stands affected by the high fire severity previously detected by field surveys and satellite images (Saulino et al. 2020). We hypothesized that the TP outbreak affected fire behavior, creating conditions for fire transition to the canopy layer by rearranging crown photosynthates, namely honeydew, along the vertical profile down to the forest floor, in both thinned and unthinned *P. pinea* stand types. Second, we related the Landsat L08 OLI/TIRS surface reflectance bands with the pre-fire monitored TP female abundance in pine stands blazed by wildfires. We hypothesized that satellite-based vegetation indices would allow us to detect TP infestation only when sooty mold colonizes black needles and branches covered by honeydew.

Methods

Study site and wildfire event

Various land uses characterize the Vesuvian landscape, including volcanic geosites, forests, farmlands, and high-density urban settlements surrounding the volcanic pediment (Fig. 1). In the summer of 2017, multiple wildfires burned 88% of the Vesuvius National Park's total forest surface. Wildfires burned approximately 600 ha of *P. pinea* forests with high severity, completely consuming soil organic horizons and surface vegetation, leading to complete overstory pine mortality (Saulino et al. 2020).

Experimental and sampling design

Two experimental designs were set up to investigate (*i*) the sensitivity of pre-fire surface reflectance bands to TP decline symptoms and (*ii*) TP outbreak effects on fire behavior in Mediterranean *P. pinea* forests (Fig. 2).

From the beginning of May 2016 to the end of March 2017, that is, before the wildfire events, field sampling was performed in *P. pinea* stands to monitor the TP abundance in six infested plots of Vesuvius National Park and one in a non-infested (control plot) coastal Paestum site (Fig. 1). In each of the six infested plots, the pre-fire TP abundance was visually assessed by field sampling in May, July, October 2016, and March 2017 on 10-cm-long terminal shoots. Surface reflectance bands were acquired from the Landsat LC08 OLI/TIRS remote sensing image collection available in Google Earth Engine (GEE), in the months of TP female abundance sampling.

In September and October 2018, 1 year after the wildfire occurrence, a post-fire sampling approach was applied to measure stand structural attributes in six 20 m-radius circular sampling plots: three in the thinned and three in the unthinned *P. pinea* stands infested with TP and severely burned in the summer of 2017. In parallel, biophysical properties of the surface and canopy fuels were assessed in two unburned plots representative of thinned and unthinned stands, located approximately 500 m from severely burned plots.

As this was an unplanned experiment, this sampling design for fire behavior modeling was intended to build a pre-fire stand structure and surface and canopy fuels in both thinned and unthinned stand types. Then, to simulate fire behavior, the measured values from three thinned and three unthinned plots were averaged to recreate the two representative stands, one thinned and one unthinned.

Satellite detection of TP decline symptoms

Toumeyella parvicornis abundance assessment

The abundance of *T. parvicornis* was assessed on four dates from May 2016 to March 2017 according to the sampling design detailed by Garonna et al. (2018) by manually counting the abundance of adult reproductive female stage. We monitored TP abundance in 6 infested plots in the *P. pinea* stands of Vesuvius National Park and 1 in a non-infested (control plot) *P. pinea* coastal stand. In each monitoring plot, the abundance of adult reproductive female stage was counted on the proximal 10 cm part

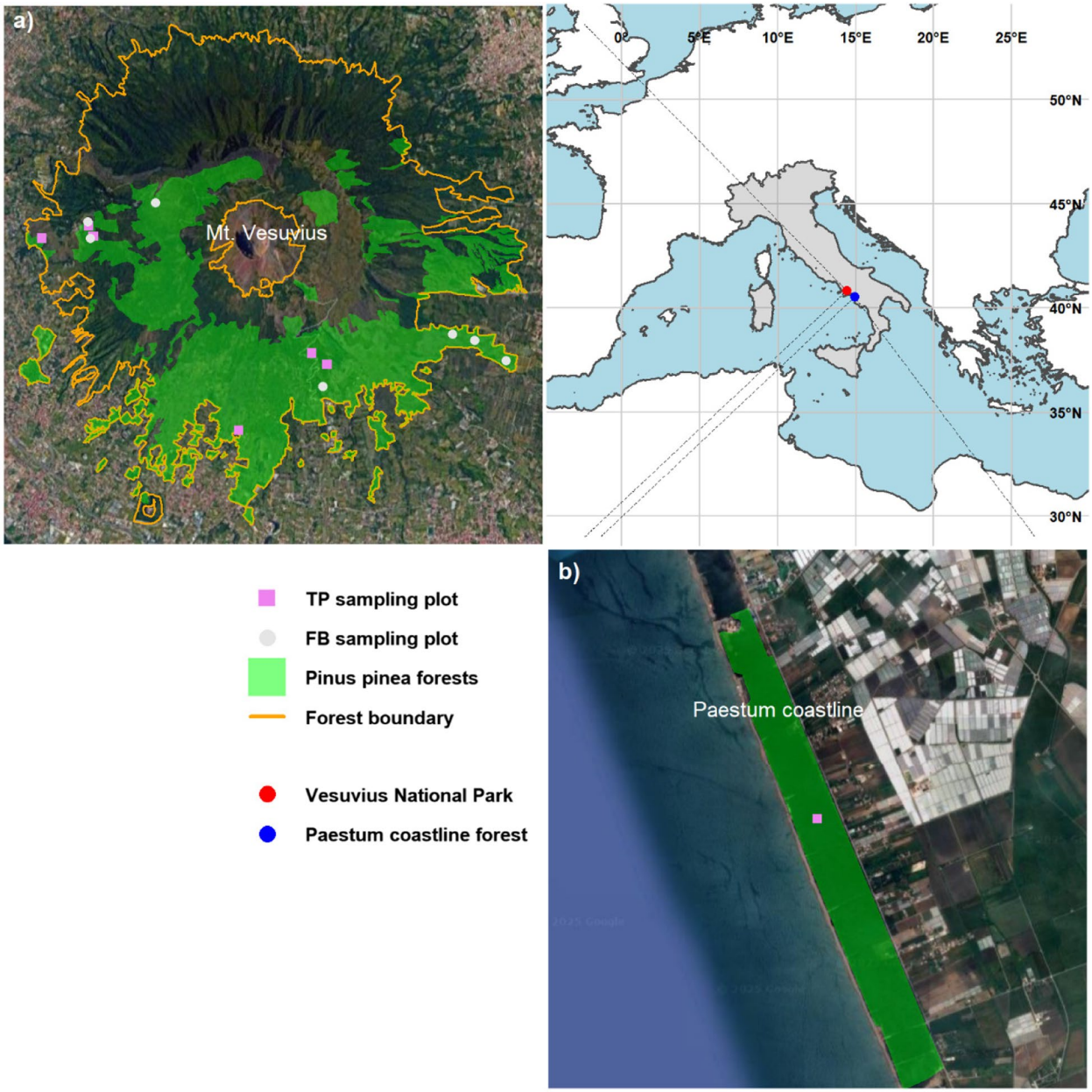

Fig. 1 Location of the study sites and field sampling plots in Vesuvius National Park (red circle marker) and Paestum coastline forest (blue circle marker) in Southern Italy. The green polygons in **a** and **b** indicate the *P. pinea* forest, while the orange line in **a** identifies the boundary of the Vesuvius National Park forests. The violet circle markers in **a** and **b** indicate the spatial position of the sampling plot of *T. parvicornis* (TP) female abundance, while the light gray circle markers in **a** indicate the location of the stand structure sampling plots in *P. pinea* stand types (unthinned and thinned) used in fire behavior (FB) simulations

of current-year terminal shoots in 30 terminal shoots of 5 dominant *P. pinea* trees randomly sampled.

As the TP completes at least three generations per year, overwintering as a mated female in reproductive diapause, the repeated measures sampling design allowed the assessment of the TP adult female abundance over four generations: the 3rd overwintering generation (2015–2016) in mid-May 2016 (spring), the 1st generation in mid-July 2016 (summer), and the 2nd generation in mid-October 2016 (fall), plus the abundance of the 3rd overwintering (2016–2017) adult female generation in mid-March 2017 (winter).

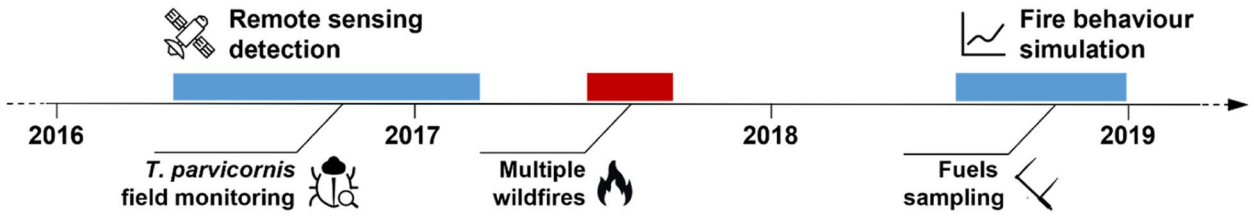

Fig. 2 Pre- and post-fire workflow to field monitoring and remotely detect *T. parvicornis* infestation and simulated fire behavior in Mediterranean *P. pinea* stand types (unthinned and thinned). Pre-fire Landsat L08 OLI/TIRS imageries were obtained in infested (local) and non-infested (relatively distant) *P. pinea* stands in months of TP monitoring from May 2016 to March 2017. After the multiple wildfire events of the 2017 summer season, stand structure and fuel samplings were carried out in burnt and unburnt (remnant) *P. pinea* stands from September to December 2018. These samplings were set to recreate the pre-fire stand structure, surface, and canopy fuel conditions used to simulate fire behavior in the unthinned and thinned stands

Table 1 Algebraic formulas and references for the two-band vegetation indices (VIs) computed using *T. parvicornis* infestation sensitive SR Landsat bands in southern Mediterranean *P. pinea* forests, where the Red, Green, NIR (near-infrared) and SWIR 2 (short wave infrared) value correspond respectively to the 30 m resolution LC08 surface reflectance bands B3 (0.53–0.59 µm), B4 (0.64–0.67 µm), B5 (0.85–0.88 µm), B7 (2.11–2.29 µm)

Vegetation index	Algebraic formula	References
Normalized Difference Vegetation Index	$NDVI = \frac{(NIR - Red)}{(NIR + Red)}$	Tucker et al., 1973
Green Normalized Difference Vegetation Index	$gNDVI = \frac{(NIR - Green)}{(NIR + Green)}$	Gitelson et al., 1996
Normalized Burn Ratio index	$NBR = \frac{(NIR - SWIR\ 2)}{(NIR + SWIR\ 2)}$	Key & Benson, 2006
Near-infrared reflectance of vegetation	$NIR_v = NDVI \bullet NIR$	Badgley et al. 2017
Green Near-infrared reflectance of vegetation	$gNIR_v = gNDVI \bullet NIR$	
Near-infrared Normalized Burn Ratio	$NIR_v = NBR \bullet NIR$	

Remote-sensed data

We used the improved Landsat Collection 2 products (USGS, 2021) in the Google Earth Engine (GEE). In GEE, we selected the Landsat 8 OLI/TIRS (LC08) Surface Reflectance Collection 2, Tier 1, Level 2 datasets (C02/T1_L2) from May 2016 to March 2017, corresponding to the dates of TP abundance field sampling. Before using C02/T1_L2 data, the surface reflectance (SR) bands were scaled by applying a scale factor of 0.0000275 and an additional offset of − 0.2 per pixel (https://www.usgs.gov/faqs/how-do-i-use-scale-factor-landsat-level-2-science-products). The quality assessment mask to exclude pixels with clouds, shadow, water, and snow was produced by applying a multi-pass algorithm called "*CFMask*" (Foga et al. 2017) and employing the Landsat quality assessment band (QA_PIXEL) (https://code.earthengine.google.com/f5c0a3979234d13313440e512c8409ae). In the GEE, the SR values of the B02-B07 bands were extracted per pixel across a stack of valid pixels (e.g., cloud and snow-free pixels) from filtered Landsat images with a sun elevation > 10°.

Satellite vegetation indices

The TP infestation-sensitive SR bands were used to compute six two-band vegetation indices (VIs) related to changes in vegetation health (Table 1). All two-band VIs are primarily based on the commonly used normalized difference VIs according to the following two algebraic formulas:

$$VI = \frac{(SR_a - SR_b)}{(SR_a + SR_b)} \quad (1)$$

$$VI_v = VI \bullet SR_{NIR} \quad (2)$$

In (1), SR_a and SR_b are two Landsat LC08 SR bands, whereas in (2), the SR_{NIR} represents a near-infrared (NIR) Landsat SR band. VI_v represents the NIR-multiplied version of the normalized difference VI.

Modeling fire behavior and its parametrization

In thinned and unthinned *P. pinea* stands, stand structure attributes were assessed in six 20 m-radius circular sampling plots, where we measured the number of trees, stem diameter at breast height (DBH, cm), total height (HT, m), and canopy base height (CBH, m). We

Table 2 Variables and values for structural and biophysical properties of the surface fuels, canopy fuels, and topographic and environmental attributes used for modeling fire behavior in thinned and unthinned *P. pinea* stands

Variable	Short description	Value		Unit
		Thinned	Unthinned	
1 h litter load	Duff and dead litter with a diameter < 0.6 cm, consisting of fallen needles, bark, and twigs	32.83	34.65	Mg ha^{-1}
1 h litter SAV[a]	The surface-area-to-volume ratio for litter with a diameter < 6 mm	7355		m^2 m^{-3}
1 h litter moisture content	Moisture content of dead litter computed on a dry basis weight	10	13	%
Fuel bed depth	Depth of dead litter fuel (< 6 mm) above the fermentation layer	15	18	cm
Moisture of extinction[a]	The threshold moisture value for litter is mainly composed of pine needles	25		%
Heat content	Gross heat of combustion (GHC) for litter, healthy needles of *P. pinea*	22,702		J g^{-1}
Canopy fuel load	Dry biomass of live needles and twigs per unit of area (< 3 cm)	2.55	2.65	kg m^2
Canopy bulk density	Dry biomass of live needles and twigs per unit of volume	0.20	0.47	kg m^3
Crown base height	Vertical distance between the ground surface and the live canopy base stratum	11.9	9.2	m
Needles moisture content[a]	Moisture content for live needles on a dry basis weight	100		%
Topographic slope	Topographic slope computed on 10 m cell resolution DEM	12.85	21.67	%
10 m open wind speed	The average value of scalar wind speed	4.92		km h^{-1}
Wind direction	The average value of the vector wind direction	337.96		degree
Wind adjustment factor	Adjust factor for the 10 m open wind speed to the midflame height below the canopy (~2 m above ground surface)	0.11	0.12	-

[a] Numerical values obtained from the literature. See the main text for further citations

measured the DBH using a tree calliper (®Haglöf Mantax), and TH and CBH of standing trees using an ultrasound digital hypsometer (®Haglöf Vertex VL402). As this experiment was unplanned, we could not determine the exact year, spatial extension, and thinning system applied in the thinned pine stands. However, we recognized the thinned stands by assessing the presence of remnant tree stumps and, consequently, by the lower tree number and basal area per ha. Owing to the structural homogeneity of single-storied *P. pinea* forests, we averaged the structural and biophysical parameters to recreate the two representative stands, one thinned and one unthinned, to predict fire behavior.

We simulated fire behavior of fuel loads and spatial arrangement conditions under thinned and unthinned stand types (Table 2). In both stands, the structural and biophysical properties of the surface fuels, canopy fuels, and topographic and environmental attributes were determined to predict fire behavior by applying Rothermel's model for fire surface spread (Rothermel 1972) and Van Wagner and Rothermel's model for crown fire initiation and spread (Rothermel 1991; Van Wagner 1977). We managed the data and simulated the fire behavior in R software (R Core Team 2024) using the "*firebehavioR*" package (Ziegler et al. 2019).

Surface fuel attributes

We computed a 1-h litter load (LL_{1h}, Mg ha^{-1}) on litter samples collected in the summer season (July–August) from both unburnt stand types. As the total energy released at the soil surface during burning reflects the heat energy content of the duff and needles burning material, 1-h litter load includes dead needles (≤ 0.6 cm) and the duff layer of partially decomposed needles, wood, and bark chips ≤ 0.6 cm. Eight litter samples (four samples per stand) were collected using PVC collars with a fixed surface area of 0.313 m^2. Next, each sample composed of litter (mainly dead pine needles) was oven-dried at 65 °C, and then the dead litter biomass was dried repeatedly until its constant weight was attained. The heat content of needles litter, specified by the amount of thermal energy released during fuel burning, was measured with Mahler's Adiabatic Bomb Calorimeter (S.D.M. Apparecchi Scientifici©, http://ariantg.com/wp-content/uploads/2017/08/Cataloguesdm.pdf) on six litter samples randomly collected from the *P. pinea* stand unburnt and uninfested by *T. parvicornis* of the Paestum coastline forest. The calorimeter was calibrated with the acid benzoic pellet, filling the bomb to 30 ± 2 bar (~ 30 atm) with oxygen. Each sample was oven-dried at 65 °C until weight loss stabilized, and then ground using a hammer mill with a 1-mm mesh size. From each milled sample, a 0.5-g aliquot was used to determine the gross heat of

combustion (GHC, J g^{-1}), representing the enthalpy of complete combustion of a fuel with all carbon oxidized to CO_2 and all hydrogen converted to H_2O.

Canopy fuel attributes

Since 1- and 2-year-old *P. pinea* needle cohorts represent the main canopy live fuel within the flaming front of the crown fire, canopy fuel attributes were assessed considering live needles and apical twig biomass at the tree and stand scales. First, live needle and twig dry biomass (NTDB, kg $tree^{-1}$) was computed at the tree scale using species-specific nonlinear allometric equations developed for the photosynthetic biomass (needles and twigs with diameters < 3 cm) of *P. pinea* trees (Cutini et al. 2013). For thinned and unthinned stands, the canopy fuel load (CFL, kg m^{-2}) was computed by summing the dry needle and twig dry biomass (NTDB, kg $tree^{-1}$) calculated for each *i*th *P. pinea* tree in the plot. Here, CFL expresses the live needle and twig fractions of the canopy fuels potentially consumed within the flaming front of a crown fire (Cruz et al. 2003).

In both thinned and unthinned stands, the canopy bulk density (CBD, kg m^{-3}) and photosynthetic dry biomass in the canopy per unit volume of the canopy (Nunes et al. 2022) were calculated as the ratio between the CFL and the stand canopy volume (SCV, m^3 m^{-2}). The SCV was calculated by summing the *i*th tree crown volume in each plot, assuming each tree crown to be a cylinder, including space. In each plot, the mean stand crown base height (CBH, m) was estimated by averaging the crown base height measured at the individual tree level.

Moisture content needles (MCN, %) of *P. pinea* were obtained (Rego et al. 2021c) and considered equal for both stand types. We selected an MNC value of 100% reported for July because this was when stand-replacing wildfires occurred in the studied stand. Although differences existed in the moisture content of needles and twigs according to age, we considered 100% as the mean value representative of MCN.

Topographic and environmental attributes

Topographic slopes were obtained from the 10 m cell-size digital elevation model (DEM) upgraded to version 1.1 (Tarquini et al. 2023), computing the slopes according to the Horn Algorithm. Time series of scalar wind speed and direction registered during July 2017 were obtained from a weather station 20 km away at 848 m a.s.l. (Agerola, 40° 38′ 48.59″ N; 14° 32′ 26.19″ E). Additionally, time series of precipitation and air temperature registered in 2017 at sub-hourly time resolution with 10-min intervals were obtained from a weather station 5 km away and at 209 m a.s.l. (Ercolano, 40° 49′ 32.00″ N, 14° 22′ 20.80″ E).

From the wind time series, we selected data registered from July 02, 2017, at 00:00:00, until July 15, 2017, at 23:50:00, the days when fires mostly spread in the pine stands. Scalar wind speed and direction data were recorded at sub-hourly time resolutions at 10-min intervals by a weather station equipped with an anemometer and wind vane sensors, both positioned at a vertical distance of 10 m above the open ground surface. The average wind speed (ws, km h^{-1}) was calculated as a simple arithmetic mean of 10 min of wind speed observations, irrespective of the wind direction, to avoid underestimating fire processes related to or dependent on wind speed (Torn and Fried 1992). The wind direction (wd, °) was calculated using vector functions (Suppl. Text S1) to avoid the challenges related to the discontinuity at 0 = 360° when the wind fluctuates around the north (Brock and Richardson 2001). Modeling surface fire behavior requires estimating the wind speed underneath the canopy, 2 m above the ground surface. To reduce the 10 m open scalar wind speed averages to the midflame height (~ 2 m), we employed the vertical wind adjustment factor (WAF) (Andrews 2012). Therefore, we calculated the sheltered WAF according to the equation developed by Andrews (2012) to consider the existing differences in the vertical and horizontal canopy structures of both pine stands.

Data analysis

To identify surface reflectance bands sensitive to TP abundance, we extracted values of the Landsat LC08 SR bands per pixel from images acquired in correspondence with TP field sampling carried out on four dates from May 2016 to March 2017. We applied principal component regression (PCR) to reduce redundant Landsat LC08 SR bands and determined how the dependent variable, TP abundance, co-varied with the independent variable, L08 SR bands. PCR was computed by employing the singular value decomposition algorithm, pooling data across sites and time, as PCR requires a large sample size to improve its performance. The *onesigma* approach was applied to identify the optimal number of PCR components according to the standard deviation of the leave-one-out ordinary cross-validation residuals and global root mean square error of prediction (RMSEP) values estimated for each PCR dimension (Hastie et al 2009). The TP infestation-sensitive SR bands were discriminated by calculating Pearson's correlation (ρ) between each variable and the components of the PCR (Husson et al. 2017), choosing the SR bands that, together with TP abundance, significantly correlated ($p < 0.05$) with the same PCR component. PCR was performed using the "*pls*" (Liland et al. 2023) R package.

We computed two-band VIs using the most sensitive Landsat LC08 SR bands to TP female abundances to detect canopy decline symptoms in infested stands. We employed a general linear model to assess the relationship between TP abundance and the two-band VIs by estimating model parameters using the ordinary least squares (OLS) procedure. In the regression model, the response variable, TP female abundance (TP_{female}, *n*), was used as a proxy for changes in tree canopy health induced by *T. parvicornis* infestation. As TP female abundance came from counting, a natural logarithmic transformation (TP abundance + 1) was used to meet the model's normality and homoscedasticity assumptions and account for zero values. Simultaneously, the two-band VIs were log-transformed (VI values + 1) as they are the algebraic ratios between the surface reflectance bands. The performance of each linear model was evaluated by assessing its accuracy using the root mean square error (RMSE) and adjusted coefficient of determination ($adjR^2$) fitting metrics. The general linear model was performed by using the "*caret*" (Kuhn 2008) R package.

Finally, we analyzed the uncertainty related to the canopy fuel attribute inputs on the simulated critical values for crown fire initiation, fireline intensity (FI, kW/m), flame length (FL, m), and surface rate of spread (ROS, m/min) computed using Van Wagner and Rothermel's models. Sources of uncertainty are related to the canopy fuel load (CFL, kg m^{-2}), bulk density (CBD, kg m^{-3}), crown base height (CBH, m), and needle moisture content (MCN, %) that significantly contribute to fire spread and its probability of transition to the tree crown (see Supp Text S2 for details). Uncertainty related to the MCN was quantified by computing critical parameters involved in crown fire ignition for 1000 generated values in the extreme range of live canopy fuel moisture conditions varying between 30 and 150% (Alexander and Cruz 2013).

Results

Fuel structure and environmental conditions preceding wildfires

Thinned and unthinned pine stands were dominated by dead litter surface fuels (1-h time lag, diameter < 0.6 cm) far from the canopy base height, 11.9 m in the thinned and 9.2 m in the unthinned stand (Table 2). While the canopy fuel load (CFL) was slightly similar, canopy bulk density (CBD) was consistently higher in the unthinned stand, with average values of 0.20 kg m^{-3} for the thinned stand and 0.47 kg m^{-3} for the unthinned stand. The latter was characterized by a significantly higher tree density and smaller trees (Suppl. Figure S1). During the wildfire days, wind mostly blew from the northwest quadrants (Suppl. Figure S2) with an average direction of 337.96° and an average arithmetic speed of 4.92 km h^{-1} (Table 2). In the month before the wildfires on July 02, 2017, rainfall was scarce, with a total of 4.6 mm occurring in the three events (Suppl. Figure S3). The latest precipitation event (1.2 mm on June 28, 2017) occurred approximately 3 days before the onset of the wildfires. During the 10 days before wildfires, the daily air temperatures ranged from 19.7 to 34.0 °C, with an average of 25.5 °C (± 0.7).

Table 3 Rothermel predicted the fire type and critical fire behavior parameters involved in crown fire initiation for thinned and unthinned *P. pinea* stands pre-fire conditions (see Table 2 for pre-fire stand conditions)

Fire behavior parameter	Thinned		Unthinned	
	Predicted	*Critical*	*Predicted*	*Critical*
Type of fire	Surface		Surface	
Fireline intensity (kW m^{-1})	176	4677	336	2619
Flame length (m)	0.8	3.9	1.1	2.9
Rate of spread (m min^{-1})	0.8	21.8	1.2	9.6

Fire behavior model

Rothermel's model predicted surface fires in both stand types infested by *T. parvicornis*. The predicted surface fire parameters required to initiate crown fires were consistently lower than the critical thresholds (Table 3). The critical fireline intensity (FLI) in the thinned stand was 4677 kW m^{-1}, approximately double that of the 2619 kW m^{-1} predicted in the unthinned stand. In contrast, the Rothermel predicted FLI was 176 kW m^{-1} in the thinned and 336 kW m^{-1} in the unthinned stand. Furthermore, the critical surface flame length (FL) was 3.8 *vs*. 2.9 m, while predicted FL accounted for 0.8 and 1.1 in thinned and unthinned stands, respectively. The predicted critical rate of spread (ROS) of 0.8 m min^{-1} in thinned stand conditions was markedly lower than the critical ROS value of 21.8 m min^{-1} required to initiate a crown fire. In parallel, in the unthinned stand, the predicted ROS of 1.2 m min^{-1} was considerably lower than the critical value of 9.6 m min^{-1}.

Uncertainty in fire behavior predictions

By keeping the needle and twig moisture (MCN) constant at 100% for each of the thousand randomly simulated canopy fuel conditions (Suppl. Figure S4), Rothermel's model predicts that only surface fires would occur in thinned *P. pinea* stands (Fig. 3). Meanwhile, 62.7% of the fires predicted were surface fires in the unthinned stand, whereas 37.3% were conditional fire types. Conditional fire indicates a type where crown fuel conditions are sufficient to support active crowning, but

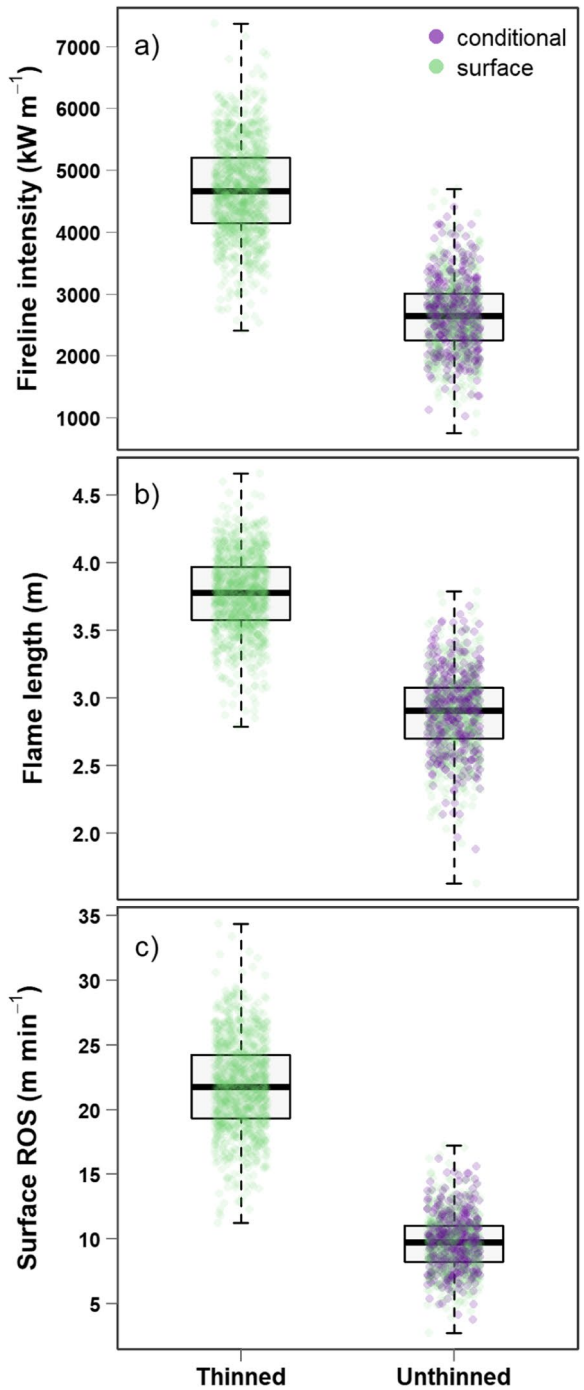

Fig. 3 Type of fire and critical values of the **a** fireline intensity (kW m^{-1}), **b** flame length (m), and **c** surface rate of spread (ROS, m min-1) in thinned and unthinned *P. pinea* stands predicted from $N = 1000$ randomly simulated canopy fuel conditions. Surface fire indicates a fire that burns fallen needles, bark, and twigs (≤ 0.6 cm), the duff layer, and plants near the surface. Conditional fire describes a condition where the crown bulk density (CBD) is sufficient to support a crown fire, and the surface fireline intensity (FLI) remains below the critical threshold required for crown ignition

surface fire intensity is below the critical threshold for crown fire initiation (Scott and Reinhardt 2001). Under these conditions, for 37.3% of conditional fires predicted in the unthinned stands, fire is expected to remain on the surface despite the crown fuels being able to sustain an active crown fire. The critical values of the fire parameters (FLI, FL, and ROS) needed for the onset of crowning were consistently higher in the thinned stand than those in the unthinned stand (Fig. 3). For thinned stand simulated canopy fuel conditions, critical values of fireline intensity (FLI) required to initiate a passive crown fire ranged from a minimum of 2409 kW m^{-1} to a maximum of 7366 kW m^{-1}, with a flame length (FL) varying in a range of 2.8 to 4.66 m and a ROS between 11.2 and 34.3 m min^{-1}. In contrast, a range of FLI between 752 and 4697 kW m^{-1}, with a flame length between 1.38 and 3.8 m and ROS between 2.8 and 17.24 m min^{-1}, were the critical values needed for the transition of the fire from the ground surface to the tree crown in the unthinned stand.

By varying the needle moisture content (MCN) within the range of 30–150% while keeping the structural arrangement of canopy fuels constant, Rothermel's model predicted conditional fires for MCN values below 54% in the thinned and below 98% in the unthinned *P. pinea* stand (Fig. 4). Conversely, surface fires were predicted for all MCN values above these two thresholds in both pine stands. In the thinned stand, the critical FLI required for crown ignition ranged between 1208 and 2228 kW m^{-1} for conditional fires and 2229 and 7953 kW m^{-1} for surface fires. Critical FL values were within a narrow range of 2.0 to 2.6 m, and the ROS values ranged from 5.6 to 10.3 m min^{-1} for conditional fires. Conversely, the FLI varied between 2.7 and 4.8 m for surface fires, and the ROS values ranged from 10.4 m min^{-1} to a maximum of 37.08 m min^{-1}. In the unthinned stand, critical FLI for crown ignition ranged from 676 to 2568 kW m^{-1} for conditional fires, whereas critical values of FL varied from 1.5 to 2.8 m and ROS from 2.48 to 9.3 m min^{-1}. Conversely, FLI varied from 2569 to 4453 kW m^{-1} for predicted surface fires, with FL values ranging from 2.9 to 3.7 m and critical ROS between 9.4 and 16.35 m min^{-1}.

Landsat SR bands sensitive to TP infestation

All SR bands, except NIR and TP, correlated significantly with the first PCR component (Fig. 5). In contrast, TP abundance and NIR, together with Green and SWIR 2, significantly correlated with the second PCR dimension. Specifically, TP abundance ($\rho = -0.75$, $p = 0.000$) and SWIR-2 ($\rho = -0.54$, $p = 0.003$) were negatively correlated, while NIR ($\rho = 0.97$, $p = 0.000$) and Green ($\rho = 0.53$, $p = 0.004$) were positively correlated with the second PCR. According to the one-sigma approach, two was

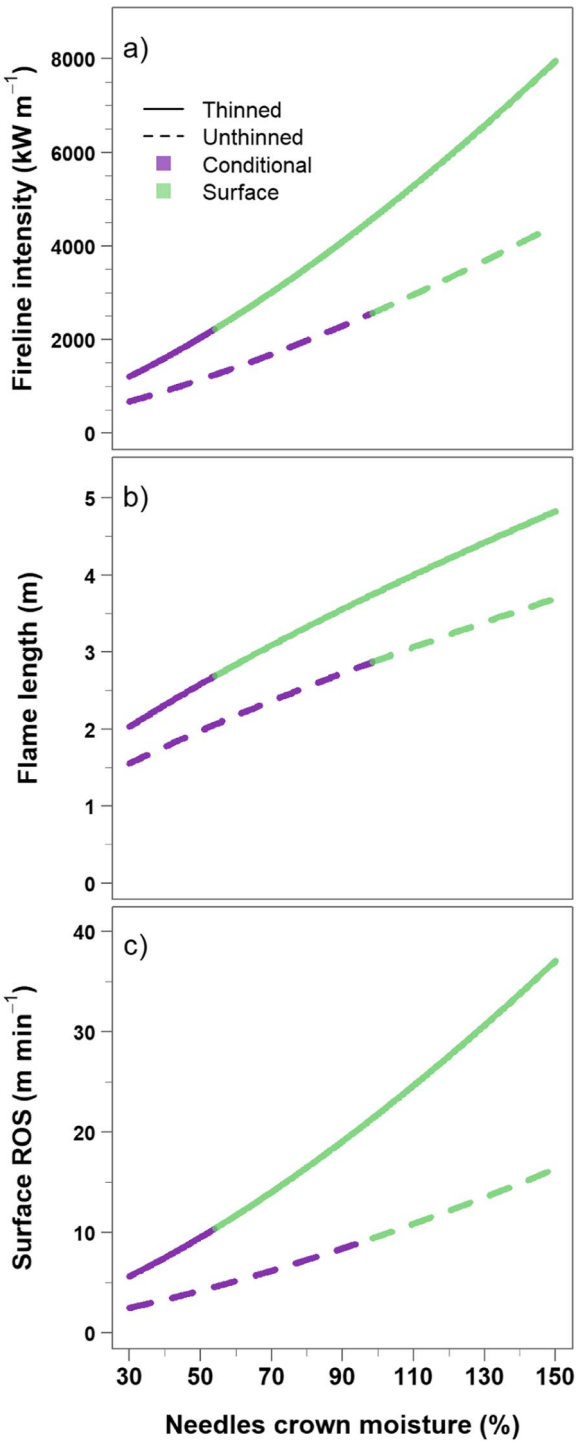

Fig. 4 Change in type of fire and critical values of the **a** fireline intensity (kW m^{-1}), **b** flame length (m), and **c** surface rate of spread (ROS, m min^{-1}) in thinned (solid line) and unthinned (dotted line) *P. pinea* stands according to the variation of a wide range in fuel moisture conditions encompassing both healthy, live, and desiccated or dead needles and twigs. For the definition of surface and conditional fire, see Fig. 3

the optimal number of dimensions in the PCR model, explaining 92% of the variance in the Landsat LC08 SR bands and producing an RMSEP of 14,4 (Suppl. Figure S5). In addition, the second PCR dimension explained 57.5% of the TP abundance variance, significantly more than the first dimension of the PCR model, which explained only 0.8% of the TP variance.

TP infestation-sensitive vegetation indices

Throughout the four TP generations, all linear relationships between female abundance and two-band vegetation indices (VIs) displayed a negative slope (Fig. 6). From the second generation in 2016 onward, the predictor variable VIs showed a significant relation (*F*-test, $P < 0.05$) with TP female abundance (Fig. 7a). Notably, NIR-multiplied VIs were significantly associated with TP abundance in the second (2016) and third (2016–2017). In contrast, standard two-band VIs were significantly related to the abundance of TP female adult stage only in the third overwintering generation (2016–2017), except for the NBR indices, which were also significantly linked to TP female abundance in the second generation (2016) (Fig. 7a).

NIR-multiplied vegetation indices were more effective in predicting the abundance of TP females than the standard version of the normalized vegetation index (VI) across the second (2016) and third (2016–2017) generations. The adjusted R-squared (adjR2) values for the standard version of the normalized two-band VIs ranged from − 0.07 to a maximum of 0.71, while the NIR-multiplied version of the two-band VIs had adjR2values ranging from 0.21 to 0.86 (Fig. 7a). Notably, all two-band vegetation indices exhibited low adjR2values during the first female generation, as observed in mid-July 2016.

Statistically significant estimated slopes (*t*-test, $P < 0.05$) were identified in the second generation (2016). Statistically significant slopes were observed in the second (2016) and third overwintering (2016–2017) generations for NBR, NIRv, gNIRv, and NBRv indices. In contrast, the NDVI and gNDVI indices were significant in the third overwintering generation (2016–2017) (Suppl. File S1). The linear models across the four TP generations exhibited RMSE values ranging from 6.4 to 15.4 (Fig. 7b). In the third overwintering generation (2015–2016), all two-band VIs showed similar RMSE values ranging from 6.5 to 7.7 while consistently increasing in the first generation in July 2016, with RMSEs between 11.0 and 13.4. Model accuracy in the second generation (October 2016) decreased to RMSE values ranging from 6.4 to 7.8 only for NIR-multiplied VIs. The RMSEs for the standard VIs were higher for the same TP generation, ranging from 8.9 to 15.5 (Fig. 7b). In the third overwintering TP generation

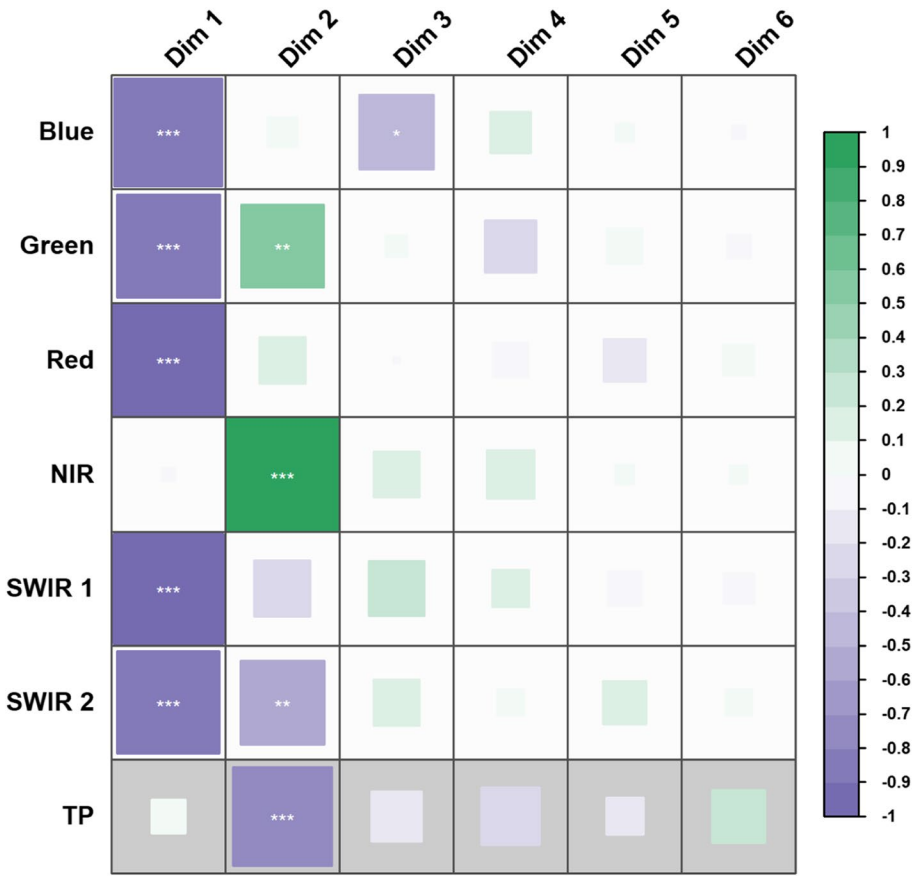

Fig. 5 Correlation plot between dimensions of principal component regression and scores of Landsat-L08 surface reflectance bands (white background) and abundance of the *T. parvicornis* (TP) female adults (gray background). White symbols ***, **, * express correlation significance *p*-value < 0.001, < 0.01, and < 0.05, respectively

(2016–2017), the accuracy of NIR-multiplied VIs was higher than that of standard VIs, with RMSE ranging from 7.7 to 9.4 and between 11.1 and 13.8.

Discussion

Fire behavior in Mediterranean pine stands infested by the alien soft-scale Toumeyella parvicornis

By simulating fire behavior across the single-storied structure of *P. pinea* stands representative of the pre-fire fuel condition, we highlighted a general pattern of predicted surface fire occurrences (low fire severity), starkly contrasting the stand-replacing wildfires (high fire severity) documented in the summer of 2017 for the same burnt stands infested by *T. parvicornis* (Saulino et al. 2020). The discrepancy between the expected and observed fire behaviors suggests that under the specified topographic and fire weather conditions, the surface fuel load's biophysical properties and spatial arrangement alone were insufficient to sustain crown fire initiation; this raises questions about the unpredictable factors that enable surface flames to overcome the wide vertical discontinuity (fuel strata gap) between the litter fuel and crown base height measured in both stand types. Along the stems, dead branches, epiphytes, lianas, likens, and bark flakes can fill the vertical discontinuity of fuels and contribute to the rise of surface flames (Cruz et al. 2003). The propagation kinematics of the flame front showed that the flames ascended from the litter to the tree stem base up to the dead and live crowns by climbing along the stems. Simultaneously, colder air masses from adjacent unburnt areas interacted with the fire, contributing to the formation of fire whirls. The images showed that epiphytes (mosses and lichens) poorly colonized the tree stems, while pruned dead branches and root-climbing liana species such as *Hedera helix* were absent, because they preferentially associate with other forest types of the Vesuvius (Saulino et al. 2023; De Marco et al. 2023). The outer stem bark may be the vector of the flames spreading upward despite its high lignin content (Rowell and Dietenberger 2013). Alternatively, we assume that the Biogenic Volatile Organic Compounds (BVOCs) emitted during the fire may have played a contingent role in

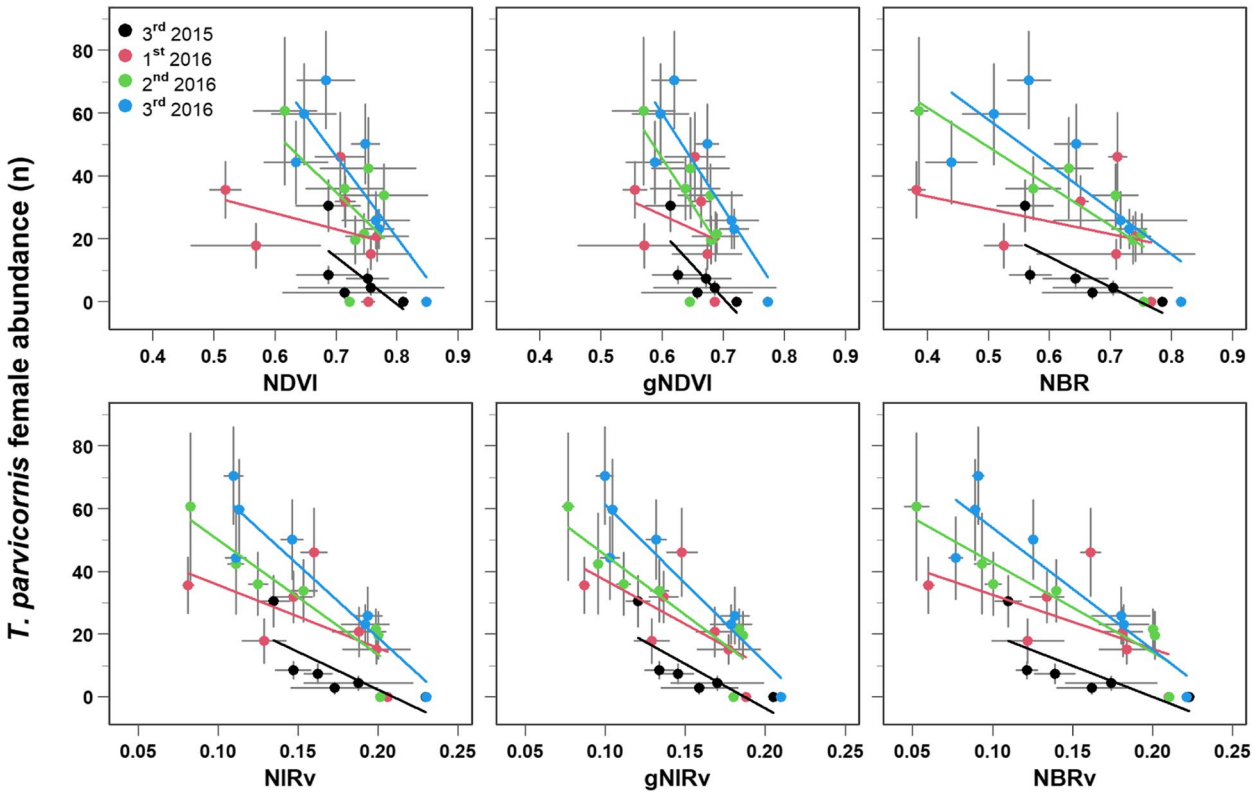

Fig. 6 Relationship between female abundance of *T. parvicornis* (n) and two-band normalized vegetation indices (see Table 1 for VIs acronyms): the 3rd overwintering generation (2015–2016) in mid-May 2016 (black circles), the 1st generation in mid-July 2016 (red circles), the 2nd generation in mid-October 2016 (green circles) and the 3rd overwintering (2016–2017) in March 2017 (blue circles). Vertical and horizontal gray lines are 1st standard deviations

the fire transition to the crown. The relationship between total BVOC content in the litter (mainly needles) of *P. pinea* and flammability has been reported in laboratory conditions (Della Rocca et al. 2017). However, in the field, the role of BVOC in the transmission of fire between fuel strata gaps has not yet been fully explored because of the difficulties in measuring them during a fire (Viegas and Simeoni 2011; Courty et al. 2014). As BVOCs have a low ignition temperature and are denser than air, some authors have suggested that when an approaching fire heat vegetation fuels, they can be emitted in the flaming front and accumulate underneath the canopy or near the ground (Barboni et al. 2011; Coudour et al. 2014).

At the time of the fire, tree stem bark smeared with dripped honeydew and sooty mold could represent proxy variables for fire severity. The honeydew excreted by TP colonies growing on the terminal shoots in the current year coated the underlying needles, branches, and stems, on which several species of sooty mold fungi grow, forming a dark layer of mycelia. Coated and opaque needles prematurely senesce, die, and drop late, inducing mortality in the proximal live branches. Consequently, in the 3-year-old dead needle cohort, phenological falling copiously in July–August was added to the premature fall of the 1- and 2-year-old brown needle cohorts, simultaneously increasing dead litter and lowering the dead canopy fuel load. The spatial rearrangement of fuels following the fall and accumulation of dead needles and honeydew dripping on the forest floor could have increased the fuel load and energy released during combustion, but not the vertical continuity. Indeed, the flame length and rate of spread in the image sequences (Suppl. Video S1) were comparable to the predicted values and were insufficient to allow the fire to spread to the crown.

Soft-scale insects synthesize high quantities of oligosaccharides to cope with phloem sap osmotic pressure, increasing the sugar concentration of the excreted honeydew deposited onto the underlying tree organ surfaces (Douglas 2006). As honeydew is water-soluble, it is easily washed off during summer rainstorms. Further, a long period of absent or scarce precipitation and high air temperature favors transient accumulation on the outermost surface of aboveground tree organs (needles, branches, and outer bark) on which colonies of black sooty mold proliferate. Under these conditions, the energy required to ignite the honeydew deposited on tree organs is

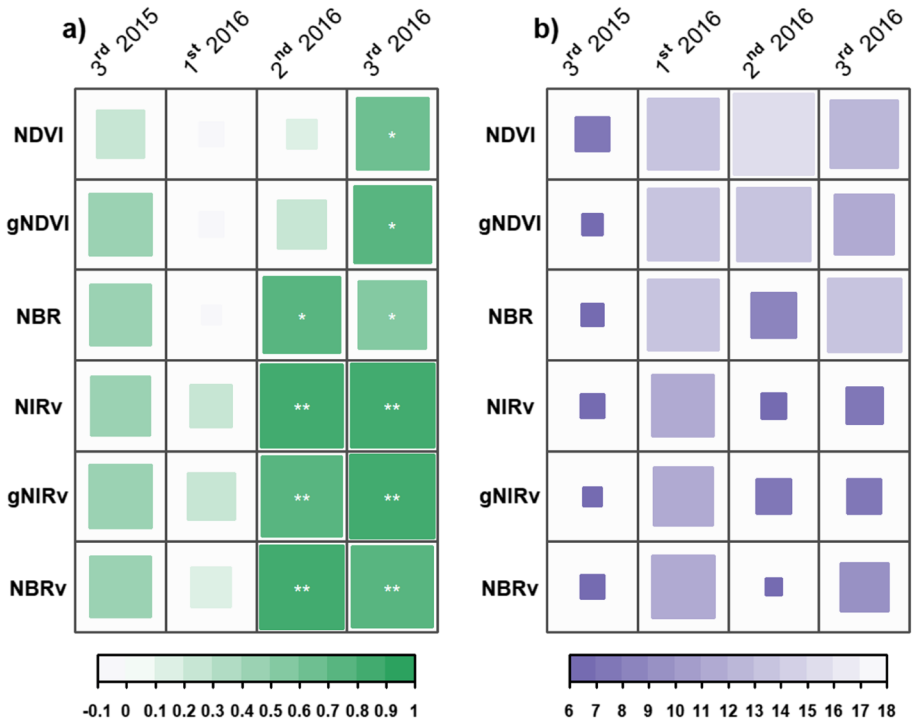

Fig. 7 Adjusted regression coefficients (**a**, *adj*R^2) and root mean square error (**b**, RMSE) estimated for each linear relationship between the TP female abundance (*n*) and two-band vegetation indices (see Table 1 for VIs acronyms) detected over *T. parvicornis* generations: the 3rd overwintering generation (2015–2016) in mid-May 2016 (spring), the 1st generation in mid-July 2016 (summer), the 2nd generation in mid-October 2016 (fall) and the 3rd overwintering (2016–2017) in March 2017 (winter). In a) white symbols ***, **, * express linear model significance *p*-value < 0.001, < 0.01, and < 0.05, respectively

expected to decrease with increased evaporative water loss. Burning the outermost bark tissue covered by honeydew, the fire climbs along the stem to the tree crown. Consequently, sugar-concentrated honeydew, combined with the flammability of *P. pinea* live needles (Della Rocca et al. 2017), probably generated an ignitable mixture with a higher heat content value, bringing canopy fine fuels to the ignition temperature; this suggests that honeydew smearing over tree components from the canopy to the underlying tree organs may have connected the live crown and litter fuel layers, amplifying fire severity and the likelihood of a crown fire. However, in the studied Mediterranean pine stands, although the phloem-feeding activity of TP redistributed along the vertical stand profile, crown photosynthates, and honeydew appeared to be the main drivers of interaction-inducing crown fires, further investigations are needed to understand the process and variables involved and their implications in modifying the dynamics of fire behavior.

Fire uncertainty and management implications

Fire behavior predicted by varying canopy fuel conditions in thinned and unthinned stands highlights that regulating stem density could have had a relatively low impact on mitigating fire severity in *P. pinea* stands infested by *T. parvicornis* outbreaks. Because pine needle moisture content (MCN) had held constant at 100%, the observed variation in critical crown fire parameters was solely related to all simulated canopy fuel conditions. Under these constraints, unlike the observed stand-replacing fires, the predicted fire types were surface fires, with conditional fires predicted only in unthinned stands. Conditional fire describes a condition in which, although the crown bulk density (CBD) is sufficient to support a crown fire, the surface fireline intensity (FLI) remains below the critical threshold required for crown ignition (Scott and Reinhardt 2001; Van Wagner 1977). Nevertheless, in both the representative pine stands, none of the surface FLIs predicted by Rothermel's model met the critical FLI values required for the onset of crowning; this suggests that the higher CBD measured in both *P. pinea* stands could have created more favorable conditions for the spread of crown fire than for its initiation. While the CBD controls the fire front's heat transfer and fire spread rate, and canopy fuel load (CFL) determines the consumption rate and heat released during fuel combustion, crown base height (CBH) and surface FLI regulate the likelihood of crown fire initiation.

Under the specified canopy fuel conditions, decreased needle and twig water content (MCN) affected the predicted fire behavior in both stand types. However, the critical fire parameters were higher than those predicted by Rothermel's model, suggesting that crown fires are unlikely to be initiated under these conditions. Nevertheless, the fire behavior parameters (FLI, FL, and surface ROS) in the unthinned pine stand showed greater sensitivity to MCN variations in the thinned stand, as conditional fires were predicted at consistently higher MCN values; this suggests that, together with CBH, the live canopy needle moisture content is relevant in controlling crown fire initiation in the studied stands. While CBH represents the vertical distance from the litter at which there is sufficient canopy fuel to sustain and propagate a fire, MCN regulates the quantity of heat of pre-ignition and residence time of the flames required for the ignition of foliar canopy fuels (Van Wagner 1977; Xanthopoulos and Wakimoto 1993).

Satellite detection of TP-infested P. pinea stand

NIR-multiplied vegetation indices accurately identified infested *P. pinea* forest stands starting from the second generation of *T. parvicornis* soft-scale insects. At the beginning of 2016, corresponding to the early stages of infestation (3rd and 1st generations of 2015 and 2016, respectively), pine trees exhibited no detectable changes in their canopy health status despite being on a declining trajectory. Symptoms of canopy health decline became detectable only from the second generation onward (October 2016). This temporal hiatus may be attributed to the fixed growth pattern of the *P. pinea* terminal shoots of *P. pinea* in the dome-shaped canopy. As *P. pinea* is characterized by a monocyclic growth pattern in which current annual shoots are preformed within the buds on the apex of the preceding year's shoots (Lanner 1976), in 2016, the rate of shoot growth of current annual shoots on the external crown and the healthy status of needles were affected solely by biotic and abiotic conditions experienced in the previous 2015 growth season, while they were unaffected by *T. parvicornis* sap-feeding activity. Consequently, in 2016, when *T. parvicornis* second generation had formed dense colonies on the current year shoot, in addition to honeydew smothering and turning black with sooty mold (Suppl. Figure S6), the underlying organs of the host tree (Bragard et al. 2022) and canopy decline symptoms became diagnostic features in *P. pinea* stand through the NIR-multiplied indices. Consequently, the NIR spectrum became sensitive to canopy decline symptoms, as the feeding activity of TP induced the premature falling of 1- and 2-year-old needles, reducing leaf area and increasing the exposure of the below-coarse branch surfaces coated with black sooty mold encrustations. The high sensitivity of NIR reflectance to blackish cover led us to infer that sooty mold is a diagnostic factor that allows the satellite detection of *P. pinea* canopy wilt symptoms related to *T. parvicornis* soft-scale outbreaks; this suggests that the higher accuracy observed in predicting TP female abundance in the second generation was related to the progressive development of sooty mold cover. However, an alternative hypothesis explaining the low detection accuracy of infested pine canopies in the first stage of infestation is the NIR reflectance spectrum of honeydew-coated needles. As honeydew consists of sugar with high reflectance in the NIR spectrum (Dull and Giangiacomo 1984), we propose that it could have enabled the detection of the first stage of infestation by keeping the NIR reflectance high and similar to that of a healthy canopy. Consequently, the absence of a significant change in the *P. pinea* canopy reflectance spectrum at the beginning of a *T. parvicornis* outbreak renders early infestation detection challenging and inaccurate.

In addition to NIR, the Green and SWIR 2 reflectance bands were sensitive to *T. parvicornis* canopy wilt symptoms, suggesting that these three bands are determinants for identifying infested *P. pinea* tree stands. As the infection progressed, before the canopy needles were dropped, they gradually turned brown and dry, probably due to changes in the needle pigment content and dehydration of tissues. Consequently, we suppose *T. parvicornis* sap feeding could induce chlorophyll degradation with repercussions in the green reflectance spectrum region (Jacquemoud and Ustin 2019a; Gitelson et al. 1996), a spectral change comparable to chlorophyll degradation in senescent needles (Jacquemoud and Ustin 2019b). Simultaneously, the feeding activity may have reduced tissue water in the needles. As the SWIR spectral region is sensitive to needle water content, dehydration following *T. parvicornis* feeding likely alters the SWIR 2 spectral responses.

Nevertheless, dehydration simultaneously alters the NIR spectral response due to the rearrangement of the mesophyll cell wall–air interfaces following a decrease in needle turgor (Jacquemoud and Ustin 2019b). Under *T. parvicornis* outbreak conditions, using the green and SWIR 2 reflectance spectrum regions and the highest-sensitivity NIR region could help improve the assessment of *P. pinea* canopy wilt symptoms. Our results partially agree with that the green, red, and NIR spectra are sensitive to black sooty mold, with NIR as a discriminant band between coated and uncoated tree leaves (Fletcher 2005). However, no difference in red surface reflectance was observed between healthy and infected conifer forests

(Olsson et al. 2012), suggesting that the role of red signals in detecting infection should be further investigated.

The higher accuracy of NIR-multiplied versions of commonly used vegetation indices for evaluating decline symptoms in pine canopies may be attributed to their remarkable ability to normalize variations in background reflectance (Badgley et al. 2017). Consequently, NIR-multiplied vegetation indices overcome mixed-pixel noise, reducing sensitivity to background contamination while emphasizing the proportion of pixel reflectance ascribable to the canopy vegetation in the pixel (Badgley et al. 2017). However, almost all satellite VIs were not invariant to changes in canopy health conditions unrelated to insect-based wilt symptoms. Hence, when canopy decline symptoms related to insect feeding activities are confused with those caused by additional factors, the reflectance data may not provide sufficient information to appropriately recognize insect outbreaks.

Conclusions

To improve fire behavior modeling, the divergence between observed and predicted fire severity in pine stands highlights the need for exploring fire-driving processes and variables related to *T. parvicornis* feeding activity on *P. pinea* trees. The high fire severity documented in thinned and unthinned stands appears consistent with a departure from known fire dynamics conditions, most probably about unknown processes and variables (e.g., BVOCs and eruptive fires) resulting from fire-insect interactions. Future research should focus on developing a more consistent and reliable fire behavior model to ensure a more comprehensive understanding of fire dynamics. Consequently, including insect-fire dynamics in fire-spread models is crucial for implementing effective fire management strategies in vulnerable ecosystems. Understanding how insect outbreaks can exacerbate fire behavior in *P. pinea* stands is essential for managing them at the local and landscape levels and developing appropriate strategies to mitigate future wildfire footprints.

The NIR, Green, and SWIR 2 reflectance bands were sensitive to *T. parvicornis* canopy wilt symptoms, suggesting that these three bands are determinants in the remote detection of infested *P. pinea* tree stands. However, as the infection progressed, symptoms of canopy health decline only became detectable from the fall generation onward when *T. parvicornis* second generation had formed dense colonies on the current year's shoot and turned black with sooty mold, the underlying organs of the host tree. Under these conditions, canopy decline symptoms become diagnostic through three NIR-multiplied vegetation indices, NIRv, gNIRv, and NBRv, computed using the most sensitive reflectance bands. Therefore, understanding how *T. parvicornis* insect-scale outbreaks modify canopy spectral signals and identifying the vegetation index using the most sensitive reflectance bands represent two essential steps toward the early recognition of *T. parvicornis* outbreaks on a large spatial scale.

Abbreviations

adjR^2	Adjusted coefficient of determination
BVOC	Biogenic Volatile Organic Compound
CBD	Canopy bulk density
CBH	Canopy base height
CFL	Canopy fuel load
DBH	Diameter at breast height
DEM	Digital elevation model
FB	Fire Behavior
FI	Fireline intensity
FL	Flame length
GEE	Google Earth Engine
gNDVI	Green Normalised Difference Vegetation Index
gNIRv	Green Near-infrared reflectance of vegetation
GHC	Gross heat of combustion
HT	Total height
MNC	Moisture content needles
NBR	Normalised Burn Ratio index
NBRv	Near-infrared Normalised Burn Ratio
NDVI	Normalised Difference Vegetation Index
NIR	Near-infrared
NIRv	Near-infrared reflectance of vegetation
NTDB	Live needle and twig dry biomass
OLS	Ordinary least squares
PCR	Principal component regression
RMSE	Root mean square error
RMSEP	Root mean square error of prediction
ROS	Surface rate of spread
SAV	Surface-area-to-volume ratio
SCV	Stand canopy volume
SR	Surface reflectance
SWIR	Short wave infrared
TP	*Toumeyella parvicornis* Cockerell
VIs	Vegetation indices
WAF	Wind adjustment factor
wd	Wind direction
ws	Wind speed

Supplementary Information

The online version contains supplementary material available at https://doi.org/10.1186/s42408-025-00382-3.

Supplementary Material 1. Suppl_Text

Supplementary Material 2. Suppl_Figures

Supplementary Material 3. Suppl_Table

Supplementary Material 4. Suppl_Video

Acknowledgements

We are grateful to Silvano Somma for his support in field sampling and to Vincenzo Topa for his assistance with the heat content assessment of pine needles. We also thank the staff at the Raggruppamento Carabinieri Biodiversità di Caserta for granting us access to the Riserva Forestale di Protezione Tirone Alto Vesuvio. We thank Mario Biafiore from Centro Funzionale Multirischi della Protezione Civile della Regione Campania for providing validated wind data. Many thanks to the two anonymous reviewers, who significantly improved the manuscript with their comments and suggestions.

Authors' contributions
LS and AS: conceptualization, investigation, methodology, and writing original draft. AS and APG: resources and supervision. LS: data curation, formal analysis, visualization, and software. LS, APG, and AS: funding acquisition. APG, FCR, AR, RS SR, AA, GL, RF, and EP: writing—review and editing. All authors read and approved the final manuscript.

Funding
This work was supported by the Technical-Scientific Agreement between the EUR S.p.A. and the Department of Agricultural Sciences of the University of Naples Federico II (CUP: E79J21005500007), granted to APG and by the Horizon Europe project "Digital tools and technology systems for the sustainable management of Mediterranean forest resources" – DIGIMEDFOR, n. 101081928 (CUP: E77G23000100006) granted to LS.

Data availability
The datasets used and analyzed during the current study are available from the corresponding author upon reasonable request.

Declarations

Ethics approval and consent to participate
Not applicable.

Consent for publication
Not applicable.

Competing interests
The authors declare that they have no competing interests.

Author details
[1]Dipartimento Di Agraria, Università Degli Studi Di Napoli Federico II, Via Università 100, 80055 Portici, Italy. [2]Centro de Ecologia Aplicada "Prof. Baeta Neves", Instituto Superior de Agronomia, Universidade de Lisboa, 1349-017 Lisbon, Portugal. [3]Laboratoire Sur Les Écosystèmes Terrestres Boréaux, Département Des Sciences Fondamentales, Université du Québec À Chicoutimi, sité, 555 Boulevard de L'Univer, Chicoutimi, QC G7H2B1, Canada.

Received: 26 February 2025 Accepted: 3 June 2025
Published: 2 July 2025

References

Alexander, M. E., and M. G. Cruz. 2013. Assessing the effect of foliar moisture on the spread rate of crown fires. *International Journal of Wildland Fire* 22:415–427. https://doi.org/10.1071/WF12008.

Andrews, P. L. 2012. Modeling wind adjustment factor and midflame wind speed for Rothermel's surface fire spread model. United States Department of Agriculture, Forest Service, Rocky Mountain Research Station GTR 266:1–39. https://doi.org/10.2737/RMRSGTR-266.

Badgley, G., C. B. Field, and J. A. Berry. 2017. Canopy near-infrared reflectance and terrestrial photosynthesis. *Science Advances* 3:e1602244. https://doi.org/10.1126/sciadv.1602244.

Barboni, T., M. Cannac, E. Leoni, and N. Chiaramonti. 2011. Emission of biogenic volatile organic compounds involved in eruptive fire: Implications for the safety of firefighters. *International Journal of Wildland Fire* 20:152–161. https://doi.org/10.1071/WF08122.

Bowman, D. M. J. S., C. A. Kolden, J. T. Abatzoglou, F. H. Johnston, G. R. van der Werf, and M. Flannigan. 2020. Vegetation fires in the Anthropocene. *Nature Reviews Earth & Environment* 1:500–515. https://doi.org/10.1038/s43017-020-0085-3.

Bragard, C., P. Baptista, E. Chatzivassiliou, F. Di Serio, P. Gonthier, J. A. Jaques Miret, A. Fejer Justesen, C. S. Magnusson, P. Milonas, J. A. Navas-Cortes, S. Parnell, R. Potting, P. L. Reignault, E. Stefani, H. H. Thulke, W. Van der Werf, A. Vicent Civera, J. Yuen, L. Zappalà, J. C. Grégoire, C. Malumphy, V. Kertesz, A. Maiorano, and A. MacLeod. 2022. Pest categorisation of *Toumeyella parvicornis*. *EFSA Journal* 20:e07146. https://doi.org/10.2903/j.efsa.2022.7146.

Brock, F. V., and S. J. Richardson. 2001. Meteorological measurement systems. Oxford University Press. https://doi.org/10.1093/oso/9780195134513.001.0001.

Butler, B. W., R. A. Bartlette, L. S. Bradshaw, J. D. Cohen, P. L. Andrews, T. Putnam, and R. J. Mangan. 1998. Fire behavior associated with the 1994 South Canyon fire on Storm King Mountain, Colorado. Res. Pap. RMRS-RP-9. Ogden, UT. United States Department of Agriculture, Forest Service, Rocky Mountain Research Station 82:009. https://doi.org/10.2737/RMRS-RP-9.

Canelles, Q., N. Aquilué, P. M. A. James, J. Lawler, and L. Brotons. 2021. Global review on interactions between insect pests and other forest disturbances. *Landscape Ecology* 36:945–972. https://doi.org/10.1007/s10980-021-01209-7.

Cervelli, E., S. Pindozzi, E. Allevato, L. Saulino, R. Silvestro, E. Scotto Di Perta, and A. Saracino. 2022. Landscape planning integrated approaches to support post-wildfire restoration in natural protected areas: The Vesuvius national park case study. *Land* 11:1024. https://doi.org/10.3390/land11071024.

Chetehouna, K., L. Courty, J. P. Garo, D. X. Viegas, and C. Fernandez-Pello. 2014. Flammability limits of biogenic volatile organic compounds emitted by fire-heated vegetation (*Rosmarinus officinalis*) and their potential link with accelerating forest fires in canyons: A Froude-scaling approach. *Journal of Fire Sciences* 32:316–327. https://doi.org/10.1177/0734904113514810.

Chomnunti, P., S. Hongsanan, B. Aguirre-Hudson, Q. Tian, D. Peršoh, M. K. Dhami, A. S. Alias, J. Xu, X. Liu, M. Stadler, and K. D. Hyde. 2014. The Sooty Moulds. *Fungal Diversity* 66:1–36. https://doi.org/10.1007/s13225-014-0278-5.

Chuvieco, E., M. L. Pettinari, N. Koutsias, M. Forkel, S. Hantson, and M. Turco. 2021. Human and climate drivers of global biomass burning variability. *Science of the Total Environment* 779:146361. https://doi.org/10.1016/j.scitotenv.2021.146361.

Clarke SR (2013) Pine tortoise scale. Forest insect & disease Leaflet 57. United States Department of Agriculture. Forest Service, p 1–8

Cooper, D. D., and W. S. Cranshaw. 2004. Seasonal biology and associated natural enemies of two *Toumeyella* spp. in Colorado. *South West Entomology* 29:39–45.

Coudour, B., K. Chetehouna, B. Conan, S. Aubrun, and J. P. Garo. 2014. Experimental investigation of the influence of geometry on gas accumulation using a V-shape forest model. In: Viegas DX (ed.), Advances in forest fire research. Imprensa da Universidade de Coimbra 2018:196–202. https://doi.org/10.14195/978-989-26-0884-6_21.

Courty, L., K. Chetehouna, J.-P. Garo, and C. Fernandez-Pello. 2014. Experimental investigations on accelerating forest fires thermochemical hypothesis. In: Viegas DX (ed.), Advances in forest fire research. Imprensa da Universidade de Coimbra 2018:203–208. https://doi.org/10.14195/978-989-26-0884-6_22.

Cruz, M. G., M. E. Alexander, and R. H. Wakimoto. 2003. Assessing canopy fuel stratum characteristics in crown fire prone fuel types of western North America. *International Journal of Wildland Fire* 12:39–50. https://doi.org/10.1071/WF02024.

Cunningham, C. X., G. J. Williamson, and D. M. J. S. Bowman. 2024. Increasing frequency and intensity of the most extreme wildfires on Earth. *Nature Ecology & Evolution* 8:1420–1425. https://doi.org/10.1038/S41559-024-02452-2.

Cutini, A., F. Chianucci, and M. Manetti. 2013. Allometric relationships for volume and biomass for stone pine (*Pinus pinea* L.) in Italian coastal stands. *iForest* 6:331–335. https://doi.org/10.3832/ifor0941-006.

De Marco, A., P. Napoletano, S. C. Panico, V. Memoli, L. Santorufo, A. G. Ruggiero, C. Colombo, R. Barile, and G. Maisto. 2023. Combined effect of black locust invasion and fire on soils of Mediterranean shrublands and pine forests. *CATENA* 220:106656. https://doi.org/10.1016/j.catena.2022.106656.

Della Rocca, G., J. Madrigal, E. Marchi, M. Michelozzi, B. Moya, and R. Danti. 2017. Relevance of terpenoids on flammability of Mediterranean species: An experimental approach at a low radiant heat flux. *iForest* 10:766–775. https://doi.org/10.3832/ifor2327-010.

Douglas, A. E. 2006. Phloem-sap feeding by animals: Problems and solutions. *Journal of Experimental Botany* 57:747–754. https://doi.org/10.1093/JXB/ERJ067.

Douglas, A. E. 2009. Honeydew. In: Encyclopedia of insects. Academic Press 1:461–463. https://doi.org/10.1016/B978-0-12-374144-8.00131-4.

Duane, A., M. Castellnou, and L. Brotons. 2021. Towards a comprehensive look at global drivers of novel extreme wildfire events. *Climate Change* 165:1–21. https://doi.org/10.1007/s10584-021-03066-4.

Dull, G. G., and R. Giangiacomo. 1984. Determination of individual simple sugars in aqueous solution by near infrared spectrophotometry. *Journal of Food Science* 49:1601–1603. https://doi.org/10.1111/J.1365-2621.1984.TB12853.X.

Fletcher, R. S. 2005. Evaluating high spatial resolution imagery for detecting citrus orchards affected by sooty mould. *International Journal of Remote Sensing* 26:495–502. https://doi.org/10.1080/01431160512331316414.

Foga, S., P. L. Scaramuzza, S. Guo, Z. Zhu, R. D. Dilley, T. Beckmann, G. L. Schmidt, J. L. Dwyer, M. Joseph Hughes, and B. Laue. 2017. Cloud detection algorithm comparison and validation for operational Landsat data products. *Remote Sensing of Environment* 194:379–390. https://doi.org/10.1016/J.RSE.2017.03.026.

Forzieri, G., L. P. Dutrieux, A. Elia, B. Eckhardt, G. Caudullo, F. Á. Taboada, A. Andriolo, F. Bălăcenoiu, A. Bastos, A. Buzatu, F. C. Dorado, L. Dobrovolný, M. L. Duduman, A. Fernandez-Carrillo, R. Hernández-Clemente, A. Hornero, S. Ionuț, M. J. Lombardero, S. Junttila, P. Lukeš, L. Marianelli, H. Mas, M. Mlčoušek, F. Mugnai, C. Nețoiu, C. Nikolov, N. Olenici, P. O. Olsson, F. Paoli, M. Paraschiv, Z. Patočka, E. Pérez-Laorga, J. L. Quero, M. Rüetschi, S. Stroheker, D. Nardi, J. Ferenčík, A. Battisti, H. Hartmann, C. Nistor, A. Cescatti, and P. S. A. Beck. 2023. The database of European forest insect and disease disturbances: DEFID2. *Global Change Biology* 29:6040–6065. https://doi.org/10.1111/gcb.16912.

Galizia, L. F., T. Curt, R. Barbero, and M. Rodrigues. 2021. Understanding fire regimes in Europe. *International Journal of Wildland Fire* 31:56–66. https://doi.org/10.1071/WF21081.

Garonna, A. P., S. Scarpato, F. Vicinanza, and B. Espinosa. 2015. First report of *Toumeyella parvicornis* (Cockerell) in Europe (Hemiptera: Coccidae). *Zootaxa* 3949:142–146. https://doi.org/10.11646/zootaxa.3949.1.9.

Garonna, A. P., A. Foscari, E. Russo, G. Jesu, S. Somma, P. Cascone, and E. Guerrieri. 2018. The spread of the non-native pine tortoise scale *Toumeyella parvicornis* (Hemiptera: Coccidae) in Europe: A major threat to *Pinus pinea* in Southern Italy. *iForest* 11:628–634. https://doi.org/10.3832/ifor2864-011.

Gausman, H. W., and W. G. Hart. 1974. Reflectance of sooty mold fungus on citrus leaves over the 2.5 to 40-micrometer wavelength interval. *Journal of Economic Entomology* 67:479–480. https://doi.org/10.1093/jee/67.4.479.

Gitelson, A.A., Kaufman, Y.J., Merzlyak, M.N. 1996. Use of a green channel in remote sensing of global vegetation from EOS-MODIS. *Remote Sensing of Environment* 58: 289–298. https://doi.org/10.1016/S0034-4257(96)00072-7.

Hastie T, Tibshirani R, Friedman J (2009) The elements of statistical learning: Data mining, inference, and prediction, 2nd edn. Springer. https://doi.org/10.1007/978-0-387-84858-7

Husson, F., S. Lê, and J. Pagès. 2017. Exploratory multivariate analysis by example using R. Chapman & Hall/CRC. https://doi.org/10.1201/b21874.

Jacquemoud, S., and S. Ustin. 2019a. Leaf optical properties in different wavelength domains. In: Leaf optical properties. Cambridge University Press 5:124–169. https://doi.org/10.1017/9781108686457.005.

Jacquemoud, S., and S. Ustin. 2019b. Variations due to leaf abiotic and biotic factors. In: Leaf optical properties. Cambridge University Press 5:195–228. https://doi.org/10.1017/9781108686457.007.

Jolly, W. M., R. A. Parsons, A. M. Hadlow, G. M. Cohn, S. S. McAllister, J. B. Popp, R. M. Hubbard, and J. F. Negron. 2012. Relationships between moisture, chemistry, and ignition of *Pinus contorta* needles during the early stages of mountain pine beetle attack. *Forest Ecology and Management* 269:52–59. https://doi.org/10.1016/j.foreco.2011.12.022.

Kane, J. M., J. M. Varner, M. R. Metz, and P. J. van Mantgem. 2017. Characterizing interactions between fire and other disturbances and their impacts on tree mortality in western U.S. forests. *Forest Ecology and Management* 405:188–199. https://doi.org/10.1016/J.FORECO.2017.09.037.

Kelly, L. T., M. S. Fletcher, I. O. Oliveras Menor, A. F. A. Pellegrini, E. S. Plumanns-Pouton, P. Pons, G. J. Williamson, and D. M. J. S. Bowman. 2023. Understanding fire regimes for a better Anthropocene. *Annual Review of Environment and Resources* 48:207–235. https://doi.org/10.1146/annurev-environ-120220-055357.

Kenis, M., M. A. Auger-Rozenberg, A. Roques, L. Timms, C. Péré, M. J. W. Cock, J. Settele, S. Augustin, and C. Lopez-Vaamonde. 2009. Ecological effects of invasive alien insects. *Biological Invasions* 11:21–45. https://doi.org/10.1007/s10530-008-9318-y.

Key, Carl H., Benson, Nathan C. 2006. Landscape Assessment (LA). In: Lutes, Duncan C.; Keane, Robert E.; Caratti, John F.; Key, Carl H.; Benson, Nathan C.; Sutherland, Steve; Gangi, Larry J. 2006. FIREMON: Fire effects monitoring and inventory system. Gen. Tech. Rep. RMRS-GTR-164-CD. Fort Collins, CO: U.S. Department of Agriculture, Forest Service, Rocky Mountain Research Station. p. LA-1-55

Knorr, W., A. Arneth, and L. Jiang. 2016. Demographic controls of future global fire risk. *Nature Climate Change* 6:781–785. https://doi.org/10.1038/nclimate2999.

Kuhn, M. 2008. Building predictive models in R using the caret package. *Journal of Statistical Software* 28:1–26. https://doi.org/10.18637/jss.v028.i05.

Lanner, R. M. 1976. Patterns of shoot development in *Pinus* and their relationship to growth potential. In Tree physiology and yield improvement – Shoot and cambial growth, ed. M. G. R. Cannell and F. T. Last, 223–243. Academic Press.

Liland, K. H., B. H. Mevik, and R. Wehrens. 2023. pls: Partial least squares and principal component regression. R package version 2:8–3.

Meigs, G. W., J. L. Campbell, H. S. J. Zald, J. D. Bailey, D. C. Shaw, and R. E. Kennedy. 2015. Does wildfire likelihood increase following insect outbreaks in conifer forests? *Ecosphere* 6:1–24. https://doi.org/10.1890/ES15-00037.1.

Misseyanni, A., A. Christopoulou, I. Kougkoulos, E. Vassilakis, and M. Arianoutsou. 2025. The impact of forest fires on ecosystem services: The case of Greece. *Forests* 16:533. https://doi.org/10.3390/f16030533.

Niccoli, F., J. P. Kabala, S. Altieri, S. Faugno, and G. Battipaglia. 2024. Impact of *Toumeyella parvicornis* outbreak in *Pinus pinea* L. forest of Southern Italy: First detection using a dendrochronological, isotopic and remote sensing analysis. *Forest Ecology and Management* 566:122086. https://doi.org/10.1016/j.foreco.2024.122086.

Nicoletti, R., L. De Masi, A. Migliozzi, and M. M. Calandrelli. 2024. Analysis of dieback in a coastal pinewood in Campania, Southern Italy, through high-resolution remote sensing. *Plants* 13:182. https://doi.org/10.3390/plants13020182.

Nunes, L., M. Pasalodos-Tato, I. Alberdi, A. C. Sequeira, J. A. Vega, V. Silva, P. Vieira, and F. C. Rego. 2022. Bulk density of shrub types and tree crowns to use with forest inventories in the Iberian Peninsula. *Forests* 13:555. https://doi.org/10.3390/f13040555.

Olsson, P. O., A. M. Jönsson, and L. Eklundh. 2012. A new invasive insect in Sweden – *Physokermes inopinatus*: Tracing forest damage with satellite based remote sensing. *Forest Ecology and Management* 285:29–37. https://doi.org/10.1016/J.FORECO.2012.08.003.

Pais, C., J. R. Gonzalez-Olabarria, P. Elimbi Moudio, J. Garcia-Gonzalo, M. C. González, and Z. J. Shen. 2023. Global scale coupling of pyromes and fire regimes. *Communications Earth & Environment* 4 (1): 267. https://doi.org/10.1038/s43247-023-00881-8.

Pausas, J. G., and J. E. Keeley. 2021. Wildfires and global change. *Frontiers in Ecology and the Environment* 19:387–395. https://doi.org/10.1002/fee.2359.

Pausas, J. G. 2022. Pyrogeography across the western Palaearctic: A diversity of fire regimes. *Global Ecology and Biogeography* 31:1923–1932. https://doi.org/10.1111/geb.13569.

Pincebourde, S., J. van Baaren, S. Rasmann, P. Rasmont, G. Rodet, B. Martinet, and P. A. Calatayud. 2017. Plant–insect interactions in a changing world. In: Adv Bot Res. Academic Press 81:289–332. https://doi.org/10.1016/bs.abr.2016.09.009.

Pyšek, P., S. Bacher, M. Chytrý, V. Jarošík, J. Wild, L. Celesti-Grapow, N. Gassó, M. Kenis, P. W. Lambdon, W. Nentwig, J. Pergl, A. Roques, J. Sádlo, W. Solarz, M. Vilà, and P. E. Hulme. 2010. Contrasting patterns in the invasions of European terrestrial and freshwater habitats by alien plants, insects and vertebrates. *Global Ecology and Biogeography* 19:317–331. https://doi.org/10.1111/j.1466-8238.2009.00514.x.

R Core Team (2024). _R: A Language and Environment for Statistical Computing_

Rego FC, Morgan P, Fernandes P, Hoffman C (2021a) Extreme fires. In: Fire science: From Chemistry to Landscape Management. Springer textbooks in earth sciences, Geography and Environment. Springer, Cham, p 175–257. https://doi.org/10.1007/978-3-030-69815-7_8

Rego FC, Morgan P, Fernandes P, Hoffman C (2021b) Fire regimes, landscape dynamics, and landscape management. In: Fire Science: From Chemistry to Landscape Management. Springer Textbooks in Earth Sciences,

Geography and Environnment. Springer, Cham, p 421–507. https://doi.org/10.1007/978-3-030-69815-7
Rego FC, Morgan P, Fernandes P, Hoffman C (2021c) Fuel dynamics and management. In: Fire science: From Chemistry to Landscape Management.Springer textbooks in earth sciences, Geography and Environment. Springer, Cham, p 363–420. https://doi.org/10.1007/978-3-030-69815-7_11
Rhodes, M. W., J. J. Bennie, A. Spalding, R. H. ffrench-Constant, and I. M. D. Maclean. 2022. Recent advances in the remote sensing of insects. *Biological Reviews* 97:343–360. https://doi.org/10.1111/brv.12802.
Roques, A., J. Shi, M. A. Auger-Rozenberg, L. Ren, S. Augustin, and Y. Q. Luo. 2020. Are invasive patterns of non-native insects related to woody plants differing between Europe and China? *Front Forests Glob Change* 2:491770. https://doi.org/10.3389/ffgc.2019.00091.
Rothermel, R. C. 1991. Predicting behavior and size of crown fires in the northern Rocky Mountains. USDA Forest Serv Intermountain Res Stn Res Pap. https://doi.org/10.2737/INT-RP-438.
Rothermel RC (1972) A mathematical model for predicting fire spread in wildland fuels, Res. Pap. United States Department of Agriculture, Intermountain Forest and Range Experiment Station, Ogden, UT, INT-115
Rowell, R. M., and M. A. Dietenberger. 2013. Thermal Properties, Combustion, and Fire Retardancy of wood. In Handbook of wood chemistry and wood composites, ed. R. M. Rowell, 127–149. Taylor & Francis Group: CRC Press.
Saulino, L., A. Rita, A. Migliozzi, C. Maffei, E. Allevato, A. P. Garonna, and A. Saracino. 2020. Detecting burn severity across Mediterranean forest types by coupling medium-spatial resolution satellite imagery and Field data. *Remote Sensing* 12:741. https://doi.org/10.3390/rs12040741.
Saulino, L., A. Rita, A. Stinca, G. Liuzzi, R. Silvestro, S. Rossi, and A. Saracino. 2023. Wildfire promotes the invasion of *Robinia pseudoacacia* in the unmanaged Mediterranean *Castanea sativa* coppice forests. *Frontiers in Forests and Global Change* 6:1177551. https://doi.org/10.3389/ffgc.2023.1177551.
Scott, J. H., and E. D. Reinhardt. 2001. Assessing crown fire potential by linking models of surface and crown fire behavior. Res. Pap. RMRS-RP-29. Fort Collins, CO. United States Department of Agriculture, Forest Service 59:29. https://doi.org/10.2737/RMRS-RP-29.
Silvestro, R., L. Saulino, C. Cavallo, E. Allevato, S. Pindozzi, E. Cervelli, P. Conti, S. Mazzoleni, and A. Saracino. 2021. The footprint of wildfires on Mediterranean forest ecosystem services in Vesuvius national park. *Fire* 4:95. https://doi.org/10.3390/fire4040095.
Tarquini S, Isola I, Favalli M, Battistini A, Dotta G (2023) TINITALY, a digital elevation model of Italy with a 10 meters cell size (version 1.1). Istituto Nazionale di Geofisica e Vulcanologia (INGV). https://doi.org/10.13127/tinitaly/1.1
Tedim, F., V. Leone, M. Amraoui, C. Bouillon, M. R. Coughlan, G. M. Delogu, P. M. Fernandes, C. Ferreira, S. McCaffrey, T. K. McGee, J. Parente, D. Paton, M. G. Pereira, L. M. Ribeiro, D. X. Viegas, and G. Xanthopoulos. 2018. Defining extreme wildfire events: Difficulties, challenges, and impacts. *Fire* 1:1–28. https://doi.org/10.3390/fire1010009.
Torn, M. S., and J. S. Fried. 1992. Predicting the impacts of global warming on wildland fire. *Climate Change* 21:257–274. https://doi.org/10.1007/BF00139726.
Tucker, C.J., Miller, L.D., Pearson, R.L., 1973. Measurement of the combined effect of green biomass, chlorophyll, and leaf water on canopy spectroreflectance of the shortgrass prairie. *Remote Sensing of Earth Resources* 2:601–627.
Tuominen J, Lipping T, Kuosmanen V, Haapane R (2009) Remote sensing of forest health. In: Peter PG (ed.), Geoscience and remote sensing. IntechOpen. https://doi.org/10.5772/8283
Turner, M. G. 2010. Disturbance and landscape dynamics in a changing world. *Ecology* 91:2833–2849. https://doi.org/10.1890/10-0097.1.
UNEP (2022) Spreading like wildfire: The rising threat of extraordinary landscape fires
Van Wagner, C. E. V. 1977. Conditions for the start and spread of crown fire. *Canadian Journal of Forest Research* 7:23–34. https://doi.org/10.1139/x77-004.
Van Wagner, C. E. V. 1993. Prediction of crown fire behavior in two stands of jack pine. *Canadian Journal of Forest Research* 23:442–449. https://doi.org/10.1139/x93-062.
Viegas, D. X., and A. Simeoni. 2011. Eruptive behaviour of forest fires. *Fire Technology* 47:303–320. https://doi.org/10.1007/s10694-010-0193-6.
Wang, D., D. Guan, S. Zhu, M. M. Kinnon, G. Geng, Q. Zhang, H. Zheng, T. Lei, S. Shao, P. Gong, and S. J. Davis. 2020. Economic footprint of California wildfires in 2018. *Nature Sustainability* 4:252–260. https://doi.org/10.1038/s41893-020-00646-7.
Xanthopoulos, G., and R. H. Wakimoto. 1993. A time to ignition–temperature–moisture relationship for branches of three western conifers. *Canadian Journal of Forest Research* 23:253–258. https://doi.org/10.1139/x93-034.
Xu, R., P. Yu, M. J. Abramson, F. H. Johnston, J. M. Samet, M. L. Bell, A. Haines, K. L. Ebi, S. Li, and Y. Guo. 2020. Wildfires, global climate change, and human health. *New England Journal of Medicine* 383:2173–2181. https://doi.org/10.1056/NEJMsr2028985.
Ziegler, J. P., C. M. Hoffman, and W. Mell. 2019. Firebehavior: An R package for fire behavior and danger analysis. *Fire* 2:1–9. https://doi.org/10.3390/fire2030041.

Publisher's Note